Crystal chemistry peculiarities of $Cs_2Te_4O_{12}$

David Hamani [a], Andreï Mirgorodsky [a], Olivier Masson [a], Thérèse Merle-Méjean [a], Maggy Colas [a], Mikhael Smirnov [b], Philippe Thomas [a],*

[a] *Laboratoire Science des Procédés Céramiques et de Traitements de Surface, UMR 6638 CNRS, Centre Européen de la Céramique, 12 rue Atlantis, 87068 Limoges Cedex, France*
[b] *Fock Institute of Physics, Saint-Petersburg State University, 1 Ulyanovskaya street, 198504 Petrodvorets, Russia*

ARTICLE INFO

ABSTRACT

The Raman and IR-absorption spectra of the $Cs_2Te_4O_{12}$ lattice are first recorded and interpreted. Extraordinary features observed in the structure and Raman spectra of $Cs_2Te_4O_{12}$ are analyzed by using *ab initio* and lattice-dynamical model calculations. This compound is specified as a caesium-tellurium tellurate $Cs_2Te^{IV}(Te^{VI}O_4)_3$ in which Te^{IV} atoms transfer their $5p$ electrons to $[Te^{VI}O_4]_3^{6-}$ tellurate anions, thus fulfilling (jointly with Cs atoms) the role of cations. The Te^{VI}–O–Te^{VI} bridge vibration Raman intensity is found abnormally weak, which is reproduced by model treatment including the Cs^+ ion polarizability properties in consideration.

© 2011 Elsevier Inc. All rights reserved.

1. Introduction

This paper reports the results of a joint experimental, *ab initio*, and lattice-dynamical model study of the electronic structure and vibrational properties of a $Cs_2Te_4O_{12}$ crystal (R-$3m/D_{3d}^5$, with $z=1$ per primitive cell [1]), which formally can be considered as $Cs_2O+Te^{IV}O_2+3Te^{VI}O_3$ complex oxide. Recently, considerable interest was manifested to this compound from the side of material science [2], which was initially provoked just by some structural peculiarity found in its lattice, namely, an unusually high symmetry of the Te^{IV} atom positions lying in the centers of quite regular $Te^{IV}O_6$ octahedrons. One more chemical peculiarity can be added to this point: the Raman spectrum of $Cs_2Te_4O_{12}$ has no feature inherent to the symmetric Te–O–Te bridge vibrations, although such bridges are the basic structural fragments of that compound and normally, in such a case, its presence should be displayed by the Raman scattering (see e.g. the case of TeO_3 [3]). The present work was aimed at understanding the origins of both the above-mentioned intriguing facts reflecting, to our belief, some sort of "anomalies" for the crystal chemistry of TeO_2–TeO_3 mixed crystalline structures and related materials to which increasing attention is currently paid. Actually, if a X_iO_j oxide is the strongest acid-former among those composing a $X_iO_j+Y_kO_l$ complex oxide, the latter is recognized as a $Y_kX_iO_{j+1}$ salt of a

(frequently hypothetical) $H_{2l}X_iO_{j+1}$ acid, and Y_kO_l as a base. Chemically, this implies that the O_l oxygen atoms *lying between atoms X and Y*, and formerly belonging to the modifier, are presently bonded to X much stronger than to Y. Consequently, there is a good reason to consider the O_l atoms as terminal ones bordering the $[X_iO_{j+1}]^{2l-}$ complex anion. The main features of its chemical constitution can be revealed from the analysis of the positions and intensities of bands in the Raman spectrum of $Y_kX_iO_{j+1}$ (see e.g. [4]). In particular, if *all the X–O bonds* are terminal (the case of isolated XO_{j+1} ortho-groups), the most intense bands in the spectrum would occupy the highest-frequency domain, and none of them would lie in the middle-frequency domain, thus indicating a "bridgeless" character of the structure. The co-existence of the X–O–X bridges and X–O terminal bonds in the body of the complex anion would be manifested by strong bands in the middle- and high-frequency parts of the Raman spectrum [4]. However, if the Y–O bonds are as strong as the X–O bonds are, the situation becomes quite equivoque since the $X_iO_j+Y_kO_l$ structure would, in fact, represent a framework in which the oxygen atoms "belong" equally to all the nearest neighbors, and no terminal bonds thus would occur. Consequently, in the case of a two-hold coordination of oxygen atoms, the Raman spectrum would be dominated by middle-frequency bands related to v_{X-O-X}^{sym}, v_{X-O-Y}^{sym} and v_{Y-O-Y}^{sym} vibrations. In other words, there would be no spectro-chemical arguments for dividing the $Y_kX_iO_{j+1}$ structure into cationic and anionic parts, and defining it as a salt. The latter situation is inherent to the crystalline structures of $Te^{IV}O_2$–$Te^{VI}O_3$ complex oxides. In those

structures, the Te^{IV} and Te^{VI} atoms lie in the positions typical to pure $Te^{IV}O_2$ or $Te^{VI}O_3$ crystalline lattices, i.e. in the apexes of essentially *anisotropic* $Te^{IV}O_4$ polyhedra (disphenoids), or in the centers of *isotropic* $Te^{VI}O_6$ coordination octahedra, respectively. In analyzing such mixed structures, one can see that, on the one hand, the Te^{IV}–O covalent bonds (close to those in the TeO_2 molecule) are shorter (and thus stronger) than those making up the $Te^{VI}O_6$ octahedra which, in such a case, can hardly be considered as *tellurate anions*; on the other hand, no $[Te^{IV}O_3]^{2-}$ *tellurite anions* (or related fragments) are present there. Thus, no *objective criteria* specifying those oxides as tellurates or tellurites can be evidenced. So the question arises: which chemical evolution would undergo a $Te^{IV}O_2$–$Te^{VI}O_3$ complex oxide when extra O atoms, brought by classical modifiers like Cs_2O, are added to it? In other words, would this compound be transformed into a *tellurite* structure or into a *tellurate* one? At this point, it can be recalled that in the initial publication on the structure of $Cs_2Te_4O_{12}$ [1], this compound was classified as "tellurite–tellurate". However, no $[Te^{IV}O_3]^{2-}$ tellurite anions can be found in its lattice. To make more extended comment on this point , we wish to notice that, as a rule (always to our knowledge), the formation of various forms of tellurium dioxides is necessarily based on the $5s$–$5p$ hybridization inside the Te^{IV} atoms, which minimizes the electron energy. As a result, $5s^2$ lone electron pair centers are displaced from their former positions coinciding with the atomic centers, and lie aside those atoms. Consequently, covalent Te^{IV}–O bonds coming from a given Te^{IV} atom are always pointed away from its lone pair thus causing the coordination polyhedron to be strongly anisotropic. Crystalline $Cs_2Te_4O_{12}$ is the only exception. In this structure, each Te^{IV} atom occupies the highest-symmetry (D_{3d}) position, and is isotropically surrounded by six oxygen atoms distanced from it by 2.104 Å, thus forming a highly symmetric and weakly bound $Te^{IV}O_6$ polyhedron existing in no other compound. One further amazing point can be found in the Raman spectrum of $Cs_2Te_4O_{12}$. In its lattice, half of oxygen atoms forms symmetric Te^{VI}–O–Te^{VI} bridges which, geometrically, are similar to the Te^{VI}–O–Te^{VI} bridges in the $Te^{VI}O_3$ lattice. Since the Raman spectrum of $Te^{VI}O_3$ is absolutely dominated by the $v_{Te^{VI}-O-Te^{VI}}^{sym}$ vibrational mode lying near 330 cm^{-1} [3], it can be thought that the homolog of that mode should be readily revealed in the Raman spectrum of $Cs_2Te_4O_{12}$. However, no strong bands below 600 cm^{-1} are seen in that spectrum (see below), thus wrongly indicating a "bridge-less" character of that compound. We wish to underline that, as a rule, the Raman spectroscopy is an efficient instrument for studying structural organization of ionic-covalent oxide crystals, glasses or ceramic compositions, which is of special importance when direct (X-ray diffraction) measurements are not possible or informative. Therefore, the surprising situation in the spectrum of $Cs_2Te_4O_{12}$ may be generally instructive for the Raman spectroscopy practice and methodology. So, when analyzing the *structural organization* and *vibrational properties* (i.e. considering a classic "structure-spectra" problem) of the $Cs_2Te_4O_{12}$ lattice, one would be faced with surprising particularities in either case, and their understanding can be of fundamental crystal chemistry interest as well as of practical importance. In this paper, we wished to clarify the origin of the both above mentioned "anomalies" by analyzing the experimental evidence jointly with the *ab initio* and lattice-dynamical model calculation data on the structure, vibrational spectra and electronic organization of the $Cs_2Te_4O_{12}$ lattice, in comparing them with those obtained for TeO_3 and α-TeO_2 lattices. The paper is organized as follows. The details of experimental and computational procedures are exposed in the next section, after which the experimental and theoretical calculation results are presented. The sections which follow them contain their analysis and discussion. First the chemical factor causing the Te^{IV} atoms to keep their $5s$ atomic orbitals intact (i.e. without undergoing the

sp-hybridization) is discussed. Subsequent to this point, the above mentioned anomaly in the Raman spectrum of $Cs_2Te_4O_{12}$ is considered. To reproduce that experimental fact within the framework of a standard model approximation, a high radial softness of the electronic shell of the Cs^+ ions was suggested, which is in line with its very high experimental polarizability. The concluding remarks are given in the last section.

2. Experiment and calculations

To synthesize crystalline $Cs_2Te_4O_{12}$ samples, the basic material, TeO_2, was prepared by decomposing the commercial ortho-telluric acid H_6TeO_6 (Aldrich, 99.9%) at 550 °C for 24 h, and heated in a stoichiometric proportion with Cs_2CO_3 (Interchim, 99+ %) at 575 °C for 5 h in a platinum crucible under O_2 atmosphere. The synthesized compound was identified from the X-ray diffraction data (powder X-ray Siemens D5000 diffractometer, Bragg–Brentano θ–2θ, Cu $K\alpha$ radiations). The Raman spectrum was recorded in the 15–980 cm^{-1} range using a Jobin–Yvon spectrometer (64000 model) equipped with a Kr$^+$ laser (647.0 nm exciting line) and a CCD detector operating in a backscattering geometry. For this, a good signal/noise ratio required two scans (during 240 s per scan). The sample focalization was done through a microscope ($\times$ 50), and the diameter of the laser spot focused on the samples was about 1 μm. Measurements were performed at a low power ($<$ 200 mW) to avoid the deterioration of the sample. The spectral resolution was about 2.5 cm^{-1} at the exciting line. The infrared spectrum was scanned on a Fourier transform spectrophotometer (Nicolet 6700) using the CsI pressed pellet technique in a range 150–1000 cm^{-1}. It was recorded in the absorbance mode. The first-principles calculations were performed to obtain self-consistent information about the structure, frequencies, symmetry, eigenvectors and IR intensities (but not Raman intensities) of the zone center vibrations of $Cs_2Te_4O_{12}$, as well as about the Te–O interatomic overlap population in various TeO_2- and TeO_3-based compounds using the same *ab initio* routine. The computational technique was based on the density functional theory (DFT) using the Becke's three-parameter hybrid nonlocal exchange functional [5] combined with the Lee–Yang–Parr gradient-corrected correlation functional B3LYP [6] through the CRYSTAL06 software [7,8]. This method has already been extensively used and proved to be reliable for description of crystalline oxide compounds with regard to structural and energy characteristics [9,10]. The lattice geometry was preliminary optimized, which was particularly important here for the calculations of vibrational frequencies as CRYSTAL06 uses the analytical first derivative of the total energy to construct the Γ-point mass-weighted Hessian matrix. Crystal frequencies were computed by diagonalising this matrix. The atomic centers have been characterized by all electrons basis sets, namely, 976631-311G* for Te, 6-31d1 for O [11] and 9766331-311G for Cs [12]. The k-point sampling was chosen to be 32 points in the irreducible part of the Brillouin zone. The LADY program (recent version of CRYME [13]) was additionally used to perform an empiric lattice-dynamical model treatment allowing us to calculate the Raman intensities of the vibrations *via* the Bond Polarizability Model (BPM) [14] in which Raman intensities are classically described as related to the polarizability variations of the vibrating system. The lattice potential function was described by a Valence Force Field (VFF) approximation whose parameters were taken from [15]. As it is implied in BPM, the polarizability of our compound was considered as the sum of the Te–O ionic–covalent chemical bond polarizabilities. The bonds were characterized by the three parameters, namely, longitudinal and transversal bond polarizability derivatives (α'_l and α'_t, respectively), complemented by parameter
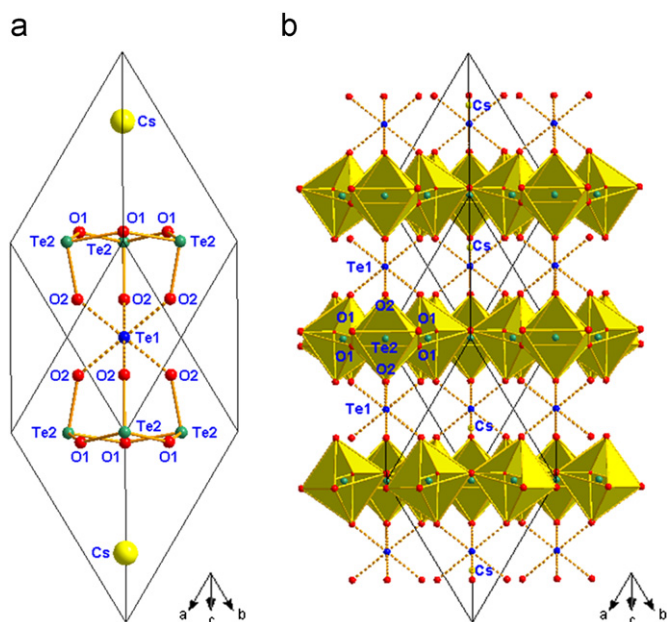
Fig. 1. (a) The atomic arrangement of the primitive cell of the $Cs_2Te_4O_{12}$ lattice. (b) The $Cs_2Te_4O_{12}$ lattice as built from Cs^+ and Te^{4+} cations separating the $[TeO_4]^{2-}_{\infty\infty}$ layer anions framed from $Te^{VI}O_6$ octahedra.
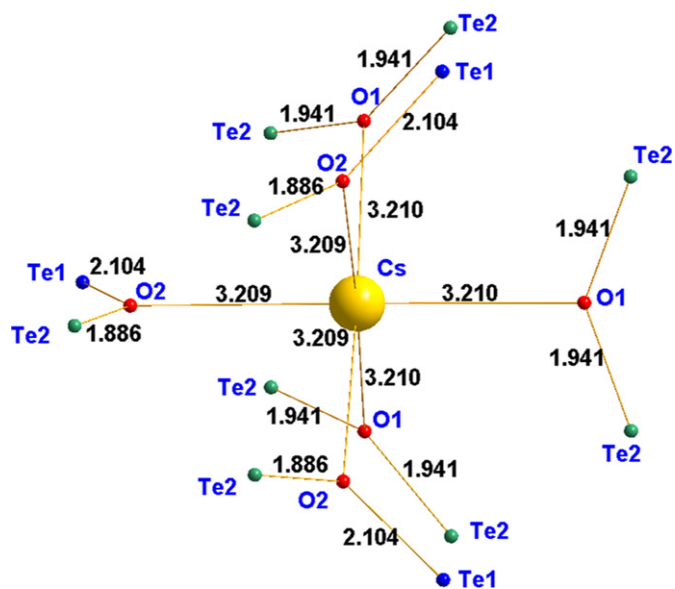

Fig. 2. Structural fragment manifesting the coordination polyhedra around Cs, O_1 and O_2 atoms.

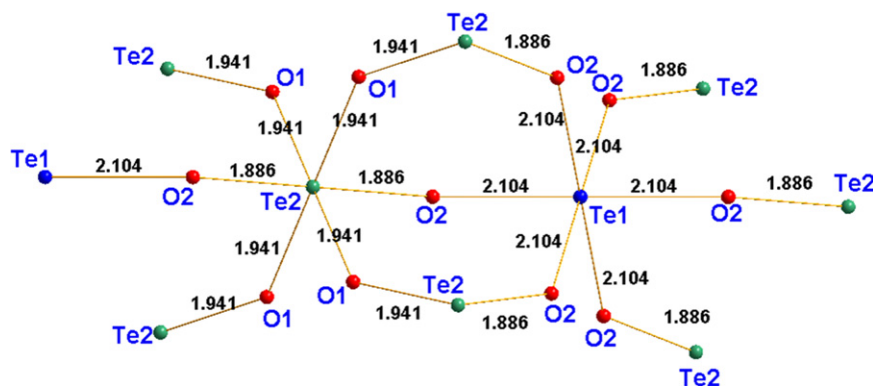**Fig. 3.** Structural fragment manifesting the coordination polyhedra around Te1 and Te2 atoms.

$\Delta = (\alpha_l - \alpha_t)/L_{Te-O}$ (see [14,16]). The two sets of those parameters were used in our calculations: standard one ignoring the role of the Cs^+ cations, and another one taking it into account (see below).

3. Results

The *ab initio* calculated optimized structure of $Cs_2Te_4O_{12}$ was in good agreement with that published in [1] so that the relevant interatomic distance differences did not exceed 5%. The atomic arrangement of the $Cs_2Te_4O_{12}$ lattice is shown in Fig. 1(a) and (b). The coordination spheres around O and Cs atoms are shown in Fig. 2, and those for atoms of Te^{IV} (labeled as Te1) and of Te^{VI} (labeled as Te2) are shown in Fig. 3. The Te–O interatomic overlap population values for TeO_2 molecule and for $Cs_2Te_4O_{12}$, TeO_3, α-, β- and γ-TeO_2 crystalline lattices are presented in Fig. 4 as the functions of interatomic bond lengths.

Those values for the Cs–O bonds (about 3.21 Å in length) in $Cs_2Te_4O_{12}$ were found to be slightly negative, thus indicating their essentially ionic character. According to the group theory analysis, the symmetry properties of the Γ-point vibrations of $Cs_2Te_4O_{12}$ (D_{3d} factor group) are as follows: $\Gamma = 5A_{1g} + 3A_{1u} + 2A_{2g} + 7A_{2u} + 7E_g + 10E_u$, the A_{1g} and E_g modes being active in Raman, and A_{2u} and E_u in infrared spectrum. The experimental Raman scattering and IR-absorption spectra of $Cs_2Te_4O_{12}$ are presented in Fig. 5(a) and (b), respectively, to which the relevant *ab initio* results are added. Each of the *ab initio* calculated IR-active modes in Fig. 5(b) is characterized there by its position, symmetry and intensity, whereas only the positions and symmetry are indicated for the calculated Raman-active modes
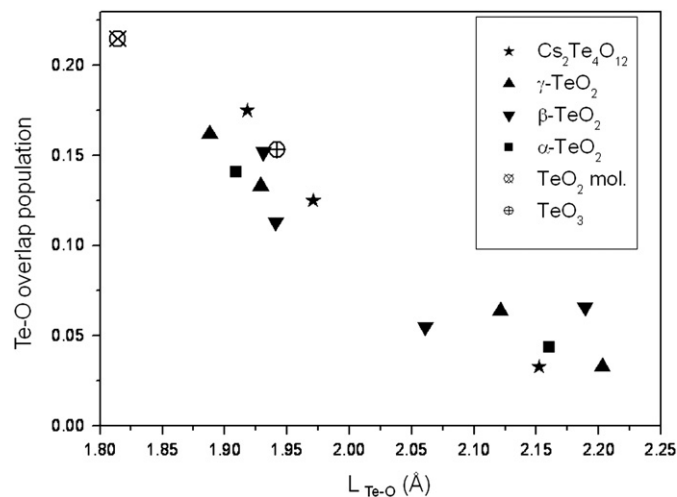

Fig. 4. The Te–O overlap population values for the $Cs_2Te_4O_{12}$, γ-TeO_2, β-TeO_2, α-TeO_2, TeO_3 lattices and for the TeO_2 molecule.
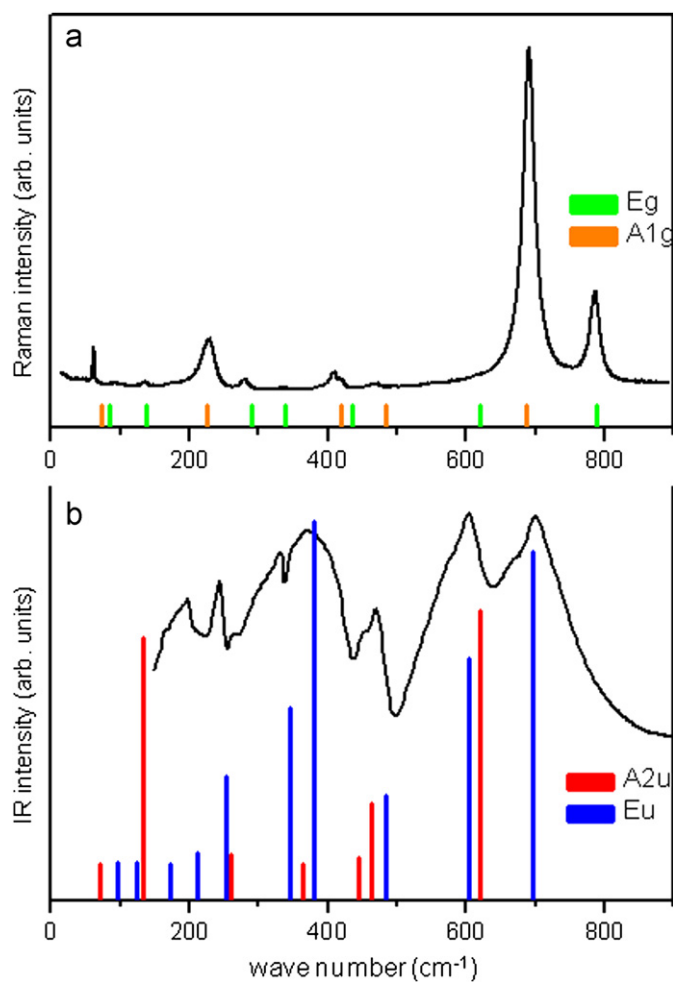
Fig. 5. Experimental spectra of (a) Raman scattering and (b) infrared absorption of powder-like samples of $Cs_2Te_4O_{12}$ complemented by the relevant *ab initio* calculations (see text).

Table 1

The BPM parameters (arbitrary units) used for the Raman scattering intensity calculations (see text and Fig. 6(a)–(b)).

Atomic pair	Interatomic distance L (Å)	α_l'	α_t'	Δ
Te_2–O_2	1.886	1.18	0.73	0.28
Te_2–O_1	1.941	1.07	0.66	0.28
Cs–O_1	3.210	0.50	0.50	0.50

in Fig. 5(a). The *ab initio* obtained eigenvectors were used for the Raman intensity estimations using the BPM approach by using the parameters presented in Table 1. The relevant results are shown in Fig. 6. The results in Fig. 6(a) ignore the effect of the Cs–O contacts; the results in Fig. 6(b) include them. Fig. 7(a)–(c) display the eigenvectors of some modes discussed below. Table 2 presents the symmetry attribution of the observed Raman-active bands using the results of the *ab initio* and empiric VFF model calculations.

4. Analysis and discussion

4.1. Lattice geometry and electronic structure

As it has been mentioned above, in the initial publication on the structure of $Cs_2Te_4O_{12}$ [1], this compound was classified as

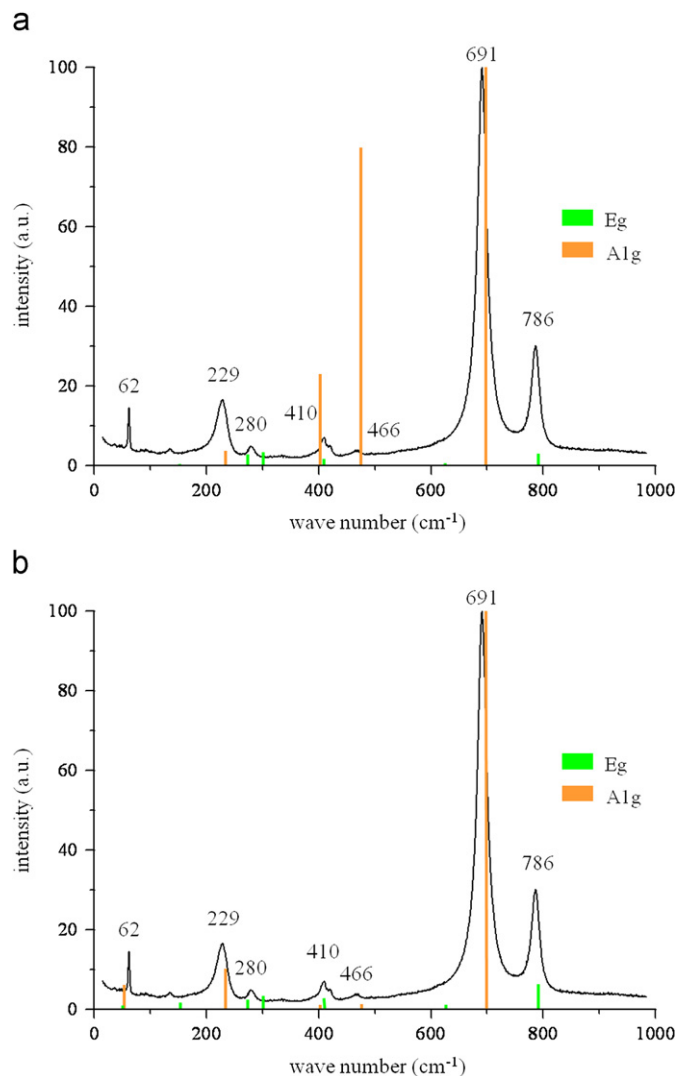**Fig. 6.** Two versions of the BPM estimations of the Raman intensity for the $Cs_2Te_4O_{12}$ lattice vibrations: (a) without including effects of the Cs-O bonds and (b) including the above mentioned effects. Experimentally observed peaks are characterized by their frequency positions.

"tellurite–tellurate". Actually, at first glance, its lattice could be regarded as containing a 3D-framework-like infinite anion (with formula $[Te^{IV}Te_3^{VI}O_{12}]^{2-}$ per primitive cell) in which *all the oxygen atoms are bridging* ones forming the Te^{IV}–O_2–Te^{VI} and Te^{VI}–O_1–Te^{VI} bridges. This would imply that of the 98 valence electrons per primitive cell, 48 are distributed between 24 Te–O bonds building one $Te^{IV}O_6$ and three $Te^{VI}O_6$ octahedra, whereas 48 electrons are located in the lone pairs of oxygen atoms, and 2 electrons form the $5s^2$ lone pair of Te^{IV}.

Such a chemical interpretation of the $Cs_2Te_4O_{12}$ structural features, at first glance, seems to be quite trivial and in good agreement with the shape of the IR spectrum in suggesting that the two strong peaks at 602 and 698 cm^{-1} in Fig. 5(b) relate to asymmetric vibrations $v_{Te-O-Te}^{as}$ of the two above mentioned types of Te-O-Te bridges, whereas strong bands in interval 350–500 cm^{-1} correspond to their symmetric v^{sym} modes. However, this assertion comes into conflict with the shape of the $Cs_2Te_4O_{12}$ experimental Raman spectrum (Fig. 5(a)). First, only very weak bands are seen in the 350–500 cm^{-1} range in which, theoretically, the $v_{Te-O-Te}^{sym}$ vibrations would dominate the spectrum. Second, a very strong band lying at 691 cm^{-1} readily indicates the occurrence of *terminal bonds*. The model calculations show
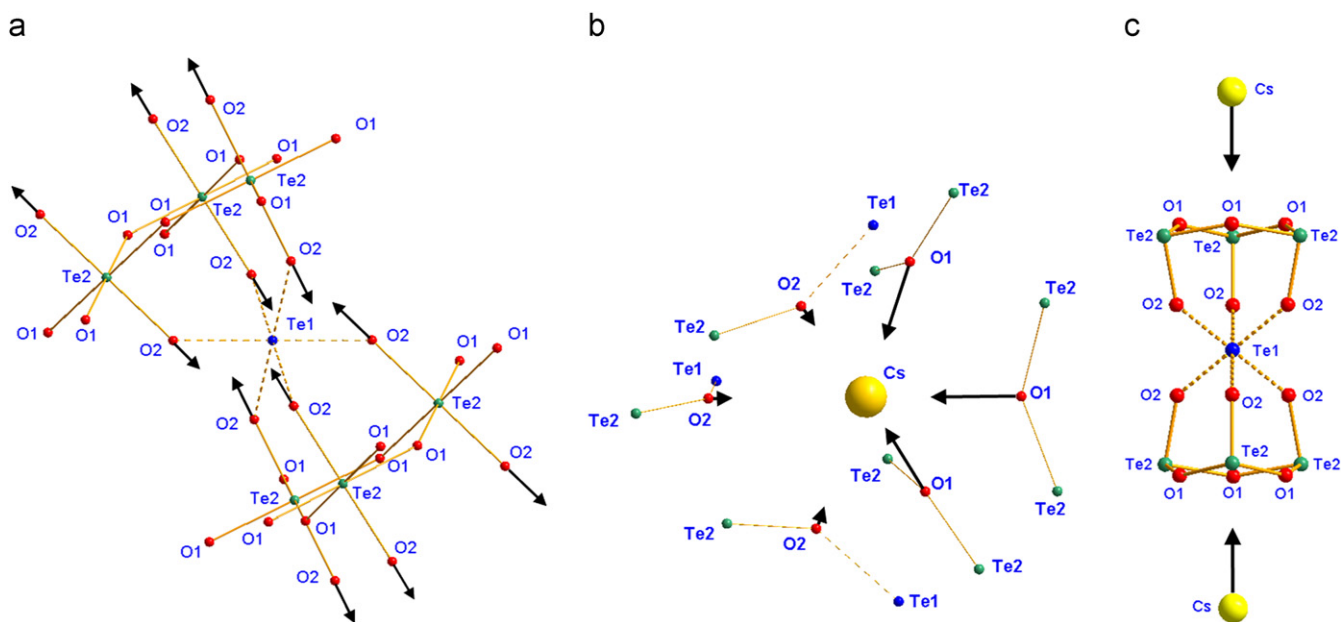
Fig. 7. Atomic displacement patterns for the vibrational modes corresponding to the bands in the Raman spectrum of $Cs_2Te_4O_{12}$ at: 691 cm^{-1} (a), 466 cm^{-1} (b) and 62 cm^{-1} (c).

Table 2
The experimental band positions (in cm^{-1}) in the Raman spectrum of $Cs_2Te_4O_{12}$ as compared with the results of *ab initio* and empiric (VFF) calculations.

Experimental	*Ab initio*	VFF
62	$73A_{1g}$	$54A_{1g}$
80	$84E_g$	$51E_g$
134	$137E_g$	$153E_g$
229	$224A_{1g}$	$234A_{1g}$
280	$291E_g$	$274E_g$
340	$339E_g$	$301E_g$
410	$420A_{1g}$	$403A1_g$
415	$435E_g$	$410E_g$
466	$484A_{1g}$	$476A_{1g}$
–	$619E_g$	$625E_g$
691	$686A_{1g}$	$698A_{1g}$
786	$788E_g$	$791E_g$

that this band corresponds to totally symmetric pure $Te^{VI}–O_2$ stretching vibrations, and none of the bands can be attributed to the $Te^{IV}–O_2–Te^{VI}$ bridge vibrations (Fig. 7(a)). Therefore, from the spectro-chemical point of view, the definition of the $Te^{IV}–O_2–Te^{VI}$ fragments as "genuine" bridges cannot be justified. The *ab initio* results (Fig. 4) strongly argue for such an issue: the overlap population value for the $Te^{VI}–O_2$ contacts (1.886 Å in length) is extremely high, whereas it is extremely low in the $Te^{IV}–O_2$ contacts (2.104 Å), thus indicating a mainly ionic nature of the latter contacts. This means that the *p*-electrons of Te^{IV} atoms are transferred to the layer-like complex tellurate anions $[Te_3O_{12}]^{6-}_{\infty\ \infty}$ which are framed of $Te^{VI}–O_6$ octahedrons, whereas the Te^{4+} and Cs^+ ions (lying between the layers) form the cationic part of the lattice. Such a chemical constitution implies that the 48 bonding electrons (per primitive cell) form 12 ordinary $Te^{VI}–O_1$ bridging bonds, and 6 double terminal $Te^{VI}–O_2$ bonds. Consequently, the compound in question should be determined as a *caesium-tellurium tellurate* whose chemical formula is $Cs_2Te^{IV}(Te^{VI}O_4)_3$.

The D_{3d} position of the Te^{IV} atoms in this compound means that their $5s^2$ electron pairs practically keep spherical shape, and are centered around the nuclei. Such a situation is extraordinary for a tellurium oxide. Actually, as a rule (i.e. always except in the case in question), to minimize the energy in the course of a Te–O

bond formation, the $5s–5p$ hybridization is initiated *inside* the Te^{IV} atom. This effect distorts the spherical shape of the $5s^2$ lone pair, and causes its center to displace out of the atomic core. It can be recalled that in a ground-state tellurium dioxide structure, α-TeO_2 paratellurite lattice, every tellurium atom can be regarded as posed inside a severely deformed $Te^{IV}O_6$ octahedron in which that atom extremely approaches (1.88 Å) two O atoms, simultaneously forming weak contacts (2.12 Å) with another oxygen couple, and has no electronic overlapping with the farthest two oxygens (2.88 Å). So, to explain why such a hybridization is absent in our case, some *external* factor preserving the $5s^2$ lone pair position and spherical configuration should be looked for, and primary attention can be paid to the surface of the $Te^{IV}O_6$ octahedra in $Cs_2Te_4O_{12}$. It must be noted that the oxygen atoms forming those surfaces (i.e. surrounding each Te^{IV}) belong to the $Te^{VI}–O_2$ nearly double bonds in which the overlap population (Fig. 4) is extremely high. In line with this fact, the Mulliken population of O_2 is found equal to 9, which, in the case of ionic–covalent bonding, indicates the practical fulfillment of the "octet rule" for oxygen atoms. In such a situation, the O_2 atoms are not predisposed to share their electron densities with the Te^{4+} ion (see the extremely low value of the overlap population for the $Te^{IV}–O_2$ bond in Fig. 4), but for this ion a symmetric electrostatic potential well in which its valence electron density distribution has to submit to the nearest environment symmetry, but not to dictate the latter like in all other cases (i.e. like in TeO_2 molecules, TeO_4 disphenoids or in $[TeO_3]^{2-}$ tellurite anions).

4.2. Raman spectra anomalies

Theoretically, the above mentioned absence of the more or less strong Raman active bands in the 350–500 cm^{-1} range could mean the absence of any "genuine" Te–O–Te bridges in the $Cs_2Te_4O_{12}$ lattice, thus implying its essentially island-type constitution, which is sharply contradicted by evidence. The results of the *ab initio* and lattice-dynamical calculations leave the situation unclear. Actually, according to them, the band at 466 cm^{-1} represents totally symmetric $Te^{VI}–O_1–Te^{VI}$ bridge vibrations, and the relevant Raman intensity estimation (Fig. 6(a)) using the "standard" BPM approach

(see the two first lines in Table 1) readily predicts their high intensities, which evidently is wrong. This situation becomes all more amazing if one takes into account that the Raman spectrum of the TeO_3 lattice (framed of symmetric Te^{VI}–O–Te^{VI} bridges with $\alpha_{Te^{VI}-O-Te^{VI}} = 138°$, and $L_{Te^{VI}-O} = 1.92$ Å) is dominated by a single strong peak at 330 cm^{-1} [3]. So, the existence of its homolog in the spectrum of the $Cs_2Te_4O_{12}$ lattice in which half of oxygen atoms forms such bridges ($\alpha_{Te^{VI}-O-Te^{VI}} = 136°$, $L_{Te^{VI}-O} = 1.94$ Å), is thought to be a certainty. This is why the lack of any strong band below 600 cm^{-1} in the experimental spectrum in Fig. 5(a) in which, moreover, the interval 300–400 cm^{-1} is empty, appears as mysterious. Then two questions rise: (i) why the frequencies of the $\nu^{sym}_{Te^{VI}-O1-Te^{VI}}$ vibrations of $Cs_2Te_4O_{12}$ are much higher than those found for $Te^{VI}O_3$? (ii) why their Raman intensity, very strong as supposed by chemical intuition and by a standard modeling, is practically vanishing in the reality? The answer to point (i) was readily deduced from the results of our lattice-dynamical model calculations. In particular, the analysis of various dynamical contributions into the frequency of the $\nu^{sym}_{Te^{VI}-O-Te^{VI}}$ mode lying at 466 cm^{-1} shows that if only Te^{VI}–O bond force constants are taken into account, this frequency drops to 310 cm^{-1}, i.e. becomes close to that found in the spectrum of the $Te^{VI}O_3$ lattice. The source of its shift to 466 cm^{-1} is the huge contribution of the forces coming from the O_1–O_1 nearest interactions. Consequently, it can be said that the frequency of about 300–330 cm^{-1} is a "genuine" frequency of the $\nu^{sym}_{O-Te^{VI}}$ vibrations of the symmetric bridges made from ordinary Te^{VI}–O bonds. The point (ii) required the analysis of the factors governing the intensity of the mode at 466 cm^{-1}. Its eigenvector (Fig. 7(b)) shows that the Cs–O_1 bond length change in the Cs–O_1–Te^{VI} fragment is strong and occurs in anti-phase relatively to Te^{VI}–O1 bond length change. This means that according to the BPM concept, the Cs–O_1 bond contributions in the Raman intensity of that mode would (partially or totally) cancel the contribution of the Te-O_1 bonds, and therefore they can account for the anomalously weak intensity of the band at 466 cm^{-1}. The BPM estimations of the Raman intensities in question showed that the addition of Cs–O_1 polarizabilty parameters to the BPM approach (the third line in Table 1) would readily cause this intensity to drop. Such a situation implies that the O_1 atom should be formally regarded as being surrounded by the three polarizable bonds, namely, the two Te^{VI}–O_1 bonds forming the Te^{VI}–O1–Te^{VI} bridge, and the Cs–O_1 bond lying nearly the plane of that bridge (see Fig. 2); in this connection, it can be noted that according to basic principles stated in [14], the in-plane vibrations of oxygen atom in a plane $X-O<^X_X$ structural fragment cannot provide a strong Raman scattering since the variation of the bond length sum, and therefore the total bond polarizabilities variation, should be small. Nevertheless, strictly speaking, the idea of the Cs–O bond polarizability, as itself, is not in line with the pure ionic nature of that bond, and the introduction of the relevant parameters in the BPM may be considered as some sort of an artificial ad hoc trick needing more justifications. Such justifications were found in analyzing the characteristics of the Raman-active modes below 250 cm^{-1} for which the model results in Fig. 6(a) are also in dramatic conflict with the experiment. Actually, in the experiment, the two low-frequency bands at 62 and 229 cm^{-1} manifest much stronger Raman intensities than those seen in the middle-frequency domain (Fig. 5(a)), whereas the model intensity pattern in Fig. 6(a) is just opposite. The ab initio results clearly show that those two bands are mainly related to the Cs–O length variations. In particular, the band at 62 cm^{-1} corresponds to the mode in which Cs atoms move along the $C3$ symmetry axis, whereas all the remaining atoms of the lattice stay immobile (see Fig. 7(c)). The band at 229 cm^{-1} is mainly related to the Cs–O_1 bond length variations in which the Cs atoms are immobile. So, the introduction of the electro-optical parameters of the Cs–O contacts (bonds) is unequivocally necessary for to put

the calculated Raman intensities of those two modes in agreement with the experimental data. By using those parameters (see Table 1), the attainment of such an agreement in our BPM calculations was automatically accompanied by the vanishing of the strong Raman intensities for all the vibrations in the 400–500 cm^{-1} interval, thus resolving the central problem—that of the abnormal weakness of the $\nu^{sym}_{Te^{VI}-O1-Te^{VI}}$ mode in the Raman spectrum of $Cs_2Te_4O_{12}$. In discussing this result, the three following points should be taken into account.

(i) As it can be seen from Fig. 7(b), the A_{1g} mode at 466 cm^{-1} corresponds to the breathings of the oxygen-made spheres surrounding the immobile Cs atoms.
(ii) The polarizability of the Cs$^+$ cation is one of the highest known for low-valence ions (see [17]); thus indicating the extraordinary softness of a "spring" between its nucleus and electronic shell.
(iii) Theoretically, the polarizability of an electronic ball bearing in its center a positive charge is proportional to the volume of that ball (see e.g. [18]).

It follows from point i that in the course of A_{1g} 466 cm^{-1} vibration, every Cs$^+$ cation is subjected by breathing tension or compression. Since this "ball" is soft (point ii), such a subjection would essentially vary its volume resulting in the variation of its polarizability (point iii), thus influencing the Raman intensity of the mode under consideration.

5. Conclusion

The joint analysis of the experimental, first-principles and empiric model results allows us to conclude the following points.

(1) $Cs_2Te_4O_{12}$ is a *tellurate structure* in which the Te^{IV} atoms transfer all their $5p$ electrons to the $[Te_3^{VI}O_{12}]^{6-}_{\infty-\infty}$ layer-like complex anions, thus playing the (unusual for them) role of cations in the tellurate compound. Their $5s^2$ lone pairs stay practically intact owing to the two factors: (i) Te^{IV} atoms are located into highly symmetric potential wells produced by O_2 atoms, and (ii) the electronic shells of O_2 atoms are saturated (due to double bonds with Te^{VI} atoms) to an extent that their electronic bonding with Te^{IV} atoms is not energetically necessary.
(2) The situation revealed in the Raman spectrum of $Cs_2Te_4O_{12}$ represents an exceptionally rare case. Actually, producing no dynamical contribution in the vibrations of the complex tellurate anions, the monovalent Cs$^+$ cations profoundly influence the polarizability properties of those vibrations, thus dramatically changing the shape of the $Cs_2Te_4O_{12}$ lattice Raman spectrum, which thus loses its true crystal chemistry informativeness. The way in which this effect was revealed and explained within the framework of a standard BPM approximation seems to be instructive and useful for understanding and interpreting the particularities of the Raman spectra of oxide materials containing heavy high-polarizable low-valence cations.

References

[1] L.O. Loopstra, K. Goubitz, Acta Crystallogr. Sect. C: Cryst. Struct. Commun. 42 (1986) 520–523.
[2] T. Siritanon, G. Laurita, R.T. Macaluso, J.N. Millican, A.W. Sleight, M.A. Subramanian, Chem. Mater. 21 (2009) 5572–5574.
[3] J. Cornette, T. Merle-Méjean, A.P. Mirgorodsky, M. Colas, M. Smirnov, O. Masson, P. Thomas, J. Raman Spectrosc. (2010) on line at wileyonlinelibrary.com, DOI 10.1002/jrs.2757.
[4] M. Soulis, A.P. Mirgorodsky, T. Merle-Mejean, O. Masson, P. Thomas, M. Udovic, J. Non-Cryst. Solids 354 (2008) 143–149.
[5] A.D. Becke, J. Chem. Phys. 98 (1993) 5648–5652.

[6] C.T. Lee, W.T. Yang, R.G. Parr, Phys. Rev. B: Condens. Matter 37 (1988) 785–789.

[7] R. Dovesi, V.R. Saunders, C. Roetti, R. Orlando, C.M. Zicovitch-Wilson, F. Pascale, B. Civarelli, K. Doll, N.M. Harrison, I.J. Bush, P. D'Arco, M. Llunell, CRYSTAL06 User's Manual, University of Torino, Torino, Italy, 2006.

[8] M. Rerat, C. Darrigan, G. Mallia, M. Ferrero, R. Dovesi, Crystal Tutorial Project on line at ⟨http://www.crystal.unito.it⟩ (2006).

[9] C.H. Hu, D.P. Chong, Encyclopedia of Computational Chemistry, John Wiley & Sons, Chichester, UK, 1998.

[10] J. Muscat, J. Wander, N.M. Harrison, Chem. Phys. Lett. 342 (2001) 397–401.

[11] C. Gatti, V.R. Saunders, C. Roetti, J. Chem. Phys. 101 (1994) 10686–10696.

[12] M.D. Towler, on line at ⟨http://www.tcm.phy.cam.ac.uk/~mdt26/basis_sets/Cs_basis.txt⟩ (1996).

[13] M.B. Smirnov, A.P. Mirgorodsky, P.E. Quintard, J. Mol. Struct. 348 (1995) 159–162.

[14] (a) M.V. Wolkenstein, C.R. Acad. Sci. URSS 30 (1941) 791–796;
(b) P. Umari, A. Pasquarello, A. Dal Corso, Phys. Rev. B: Condens. Matter 63 (2001) 094305.

[15] A.P. Mirgorodsky, T. Merle-Méjean, P. Thomas, J.C. Champarnaud-Mesjard, B. Frit, J. Phys. Chem. Solids 63 (2002) 545–554.

[16] M. Smirnov, S. Sukhomlinov, A.P. Mirgorodsky, O. Masson, E. Bechade, M. Colas, T. Merle-Méjean, I. Julien, P. Thomas, J. Raman Spectrosc. 41 (2010) 1410–1417.

[17] R.D. Shannon, R.X. Fisher, Phys. Rev. B: Condens. Matter 73 (2006) 235111.

[18] P. Politzer, P. Jin, J.S. Murray, J. Chem. Phys. 117 (2002) 8197–8202.